Physics of Fluids

On the kinetics of chemical reactions at the detonation of organic high explosives

Cite as: Phys. Fluids **34**, 087113 (2022); https://doi.org/10.1063/5.0095053
Submitted: 08 April 2022 • Accepted: 19 July 2022 • Accepted Manuscript Online: 19 July 2022 • Published Online: 10 August 2022

N. P. Satonkina and D. A. Medvedev

View Online Export Citation CrossMark

ARTICLES YOU MAY BE INTERESTED IN

Design optimization for Richtmyer–Meshkov instability suppression at shock-compressed material interfaces
Physics of Fluids **34**, 082109 (2022); https://doi.org/10.1063/5.0100100

Ignition and deflagration-to-detonation transition modes in ethylene/air mixtures behind a reflected shock
Physics of Fluids **34**, 086105 (2022); https://doi.org/10.1063/5.0103013

Large-eddy simulation of the compressible flows around a wavy-axis square cylinder
Physics of Fluids **34**, 086107 (2022); https://doi.org/10.1063/5.0102185

APL Machine Learning
Open, quality research for the networking communities
Now Open for Submissions
LEARN MORE

AIP Publishing

© 2022 Author(s).

Physics of Fluids ARTICLE scitation.org/journal/phf

On the kinetics of chemical reactions at the detonation of organic high explosives

Cite as: Phys. Fluids **34**, 087113 (2022); doi: 10.1063/5.0095053
Submitted: 8 April 2022 · Accepted: 19 July 2022 ·
Published Online: 10 August 2022

View Online Export Citation CrossMark

N. P. Satonkina[1,2,a)] and D. A. Medvedev[1,2]

AFFILIATIONS

[1]Lavrentyev Institute of Hydrodynamics SB RAS, pr. ac. Lavrentyeva, 15, Novosibirsk 630090, Russia
[2]Novosibirsk State University, Pirogova str., 1, Novosibirsk 630090, Russia

[a)]Author to whom correspondence should be addressed: snp@hydro.nsc.ru

ABSTRACT

The model of electrical conductivity developed earlier allows one to use electrical properties as a tool for the diagnostics of the reaction zone at the detonation of organic high explosives. The comparison of experimental data on electrical conductivity with both the results of experimental research and numerical modeling using Arrhenius kinetics is carried out. The contradiction of the thermal concept of the mechanism of the development of a chemical reaction during detonation is clearly demonstrated. An alternative based on the ideas of A. N. Dremin, J. J. Dick, C. S. Coffey, and F. E. Walker is discussed.

Published under an exclusive license by AIP Publishing. https://doi.org/10.1063/5.0095053

I. INTRODUCTION

The detonation wave consists of the shock front, the adjacent chemical peak (or von Neumann peak) where chemical reactions occur, and the Taylor rarefaction wave separated from the chemical peak by the Chapman–Jouguet point (CJ-point) where the velocity of products is equal to the local speed of sound. In the Zeldovich–von Neumann–Doering (ZND) theory,[1–3] the chemical reactions are completed in the CJ-point.

The interest in the reaction zone kinetics at the detonation of condensed high explosives remains high for decades. In the last few years, new calculation methods including hybrid ones arose thanks to the intensive development of computation tools. These methods are able to predict some technically important properties. However, the details of the kinetics are still questionable.

At present, the theoretical description of the state of matter in the reaction zone of the detonation wave is complicated. It is not a solid, not a liquid, not a gas, and not a plasma. The material with a density of about 3 g/cm^3 is under the pressure of several tens of GPa and the temperature of 3000–4000 K. The concentration of atoms is about $3/(M_C/N_a) \approx 10^{23}$ cm^{-3}, the average interatomic distance is $1\,\text{cm}/\sqrt[3]{10^{23}} \approx 2 \times 10^{-8}$ cm. If free electrons exist in such a medium, their mean free path would be $\lambda \sim 3 \times 10^{-8}$ cm, which is nearly the interparticle distance. The De Broglie wavelength for an electron is $h/mV \sim 10^{-7}$ cm. Hence, there are no small parameters that could be neglected in the description of the detonation wave. Under such conditions, it is hard to single out the defining processes, and the first-principles simulation looks the most promising.

According to the generally accepted understanding, the chemical reaction in a detonation wave starts within the multiple local non-uniformities with elevated temperatures, usually called hot spots.[4–19]

Among the various mechanisms capable of generating hot spots under shock impact, the collapse of pores is regarded as one of the most probable scenarios.[6–9] In a number of papers, such collapse is treated numerically, usually starting from geometrically regular voids. In order to understand the physics of the collapse, experimental and numerical studies of void deformation in an inert material (PMMA) were performed for shocks of a different magnitude—from weak ones to those typical for detonation waves.[20] In Ref. 19, the reaction in voids in TATB (triaminotrinitrobenzene) and HMX (cyclotetramethylene-tetranitramine) was modeled at different shock pressures P_S. The dependence of critical pore size on P_S was obtained.

Other non-uniformities can be considered as hot spot precursors as well. A review of the influence of the crystal defects on the sensitivity of the energetic materials is presented in Ref. 15. In Ref. 16, structural non-uniformities were considered, which can lead to ignition under shock waves. In Ref. 17, shocks in TATB were modeled using molecular dynamics. Nanometer-scaled shear bands were found in which the reaction barrier was somewhat lower, which should favor the ignition. In Ref. 18, to describe the initiation of the explosive, a multiscale model was proposed incorporating the range from the

Published under an exclusive license by AIP Publishing

molecular level to macroscale, taking the material structure into account. Other multiscale models were considered in Refs. 7 and 9.

The kinetics is interesting, first of all, from the practical point of view, to predict such an important property of high explosive (HE) as its sensitivity. This sensitivity depends on several factors such as the structure of molecule and grain size. The proposed kinetics is often verified by the known properties of the shock-wave sensitivity or impact sensitivity.

In Ref. 21, the impact sensitivity was simulated using the quantum approach. The thermal explosion is calculated for PETN (pentaerythritol tetranitrate), HMX, RDX (cyclotrimethylene trinitramine), and TNT (trinitrotoluene) with good agreement with experimental data. Similar results on the impact sensitivity were obtained in Ref. 22. Using the nonstationary theory of the density functional, the molecules of RDX, HMX, CL-20 (hexanitrohexaazaisowurtzitane), PETN, and LLM-105 (2,6-diamino-3,5-dinitropyrazine-1-oxide) were investigated in the basic singlet state after the electron excitation. In Ref. 23, a simple way was proposed to estimate the impact sensitivity from the chemical formula and the formation enthalpy of HE. The theoretical approach was proposed in Ref. 24 to quantitatively estimate the impact sensitivity based on the criteria obtained for the solid state, including the inception pressure, the average number of electrons per atom, the crystal morphology, the energy content, and the melting temperature. Twenty four substances were considered, and the scatter was about 20%. A thorough investigation was performed in Ref. 25 to elucidate the sensitivity mechanism of PETN with the groups –CH, $–CNH_2$, $–CNH_3X$, $–CCH_3$, and –PO implanted into the molecule. The results were used to carry out reactive molecular dynamic simulations. The authors note that the anisotropy of the shock-wave sensitivity of a PETN single crystal is determined not only by dislocations and unhindered slips in certain directions but also by the important role of hydrogen bonds in crystals. In Ref. 26, the transition to detonation was investigated by reactive molecular dynamic simulations with a semi-empirical description of interatomic bonds at low load pressure. The speed of the transition to a thermal explosion was obtained for ETA (erythritol tetranitrate), ETN (erythritol tetranitrate), PETN, RDX, and HMX as a function of the initial temperature and pressure.

In Ref. 27, the discrete Boltzmann method was used to simulate unsteady detonation. In Ref. 28, the improved thermodynamically consistent model of a reactive flow was proposed for the investigation of the hydrodynamic detonation of solid high explosives. The model reproduces well the important parameters of detonation flows. In Ref. 29, the reaction zone at the nitromethane detonation was simulated by EXPLO5. Two reaction stages were observed: the fast reaction (5–10 ns) that is followed by a slow decrease in pressure and the slow reaction that terminates after about 50–60 ns at the Chapman–Jouguet point. In Ref. 19, the influence of five global kinetics models on the hot spot dynamics was investigated. The hot spots are produced by the collapse of voids in HMX. It was shown that the question of the appropriate kinetics model remains unsolved.

The course of a chemical reaction and the sequence of the bond breaking in a molecule of HE is determined by many factors. For instance, the breakup of a $N–NO_2$ bond in the molecule of RDX with a formation of a single NO_2 radical is a primary act under the action of laser radiation with minimum power.[30,31] Under a powerful action on the molecule, a fast breakdown of the ring is a prevailing act with a breaking of C–N bonds despite the fact that the breaking of the $N–NO_2$ bond is energetically more favorable.[30,32]

Interesting results were obtained in Ref. 33 where first principles reactive molecular dynamics simulations of high-velocity bimolecular collisions of PETN were performed. The authors conclude that chemical reactions are controlled by the dynamics, which include mechanical deformations, steric effects, thermal oscillations (in the case of the C–H bond breakup), and the non-thermal excitations localized in oscillation modes.

While being in good agreement with experimental data, different models contradict each other in detail. It is impossible to explain in the framework of one available model the whole complex of physical phenomena, such as the anisotropy of the shock-wave sensitivity of a HE single crystal, the non-monotonic dependence of the shock-wave sensitivity on the grain size,[34] the distribution of the electrical conductivity, and the rapid formation of penetrating conductive structures. The detailed kinetics of the reaction zone was proposed in Refs. 35 and 36, as shown in Fig. 1, top. Using the simulation of macroparameters, the authors developed the reaction sequence where the formation of water, CO_2, and N_2 occur simultaneously, and the formation of condensed carbon finishes the reaction. In the bottom part of Fig. 1,

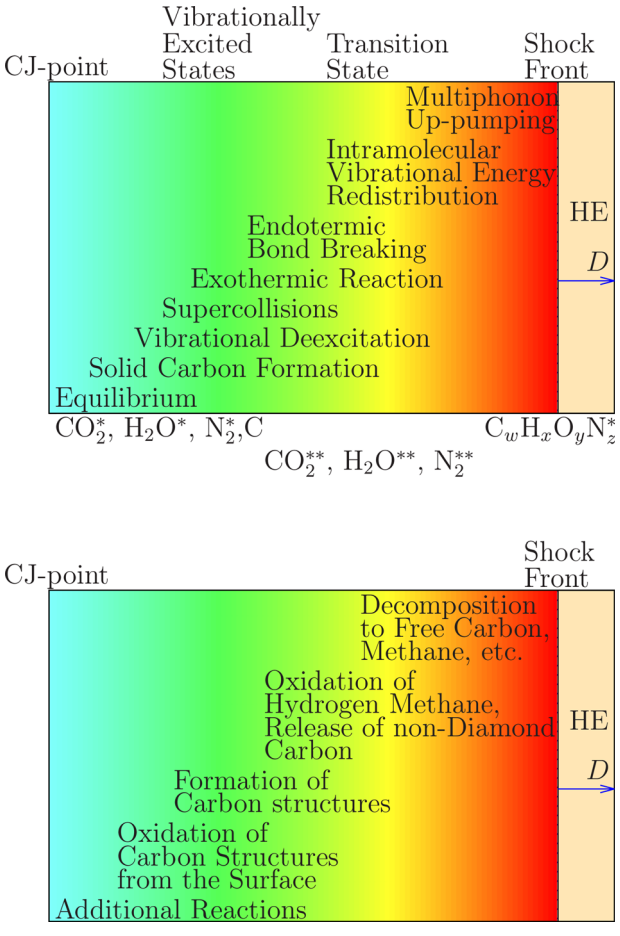

FIG. 1. Top: Unsteady ZND kinetics model of Tarver.[35] Bottom: Kinetics model of Anisichkin based on the investigation by the tracer atoms method and the behavior of organic substances at the shock load.[37]

Published under an exclusive license by AIP Publishing

the kinetics is shown developed by the tracer atom method.[37] In contrast with the model of Tarver, the release of "free" carbon atoms occurs immediately after the front. In Ref. 38, quantum molecular dynamic simulations were performed. The two-stage reaction mechanism at the detonation of the RDX crystal was obtained. The formation of N_2 and H_2O takes place at 10 ps and is accompanied by the delay in the formation of CO molecules. The growth of a carbon cluster after the shock was obtained.

Thus, the contradictions listed above demonstrate the absence of a commonly approved kinetics model and essential method difficulties with the experiment. This is caused mainly by the absence of an experimental tool suitable for the detailed investigation of the reaction zone. The aggressive medium of the chemical peak together with the short duration of the process restricts significantly the circle of available methods. The analysis of preserved detonation products or the method of tracer atoms[37] provides only integral information. The interferometer investigations[39] are not related to the chemical state of the substance. The results of the ultrafast absorption spectroscopy[40] are hard to interpret.

The main requirement for the development of the detonation kinetics of condensed HE is the availability of adequate precise information. The only source of such information is the experiment. In this paper, the novel diagnostic method through electrical conductivity is used as an experimental method sensitive to the chemical state and provides information in process.

II. TOOL FOR THE REACTION ZONE DIAGNOSTICS AT THE DETONATION

The method of experimental investigation of electrical conductivity is described in Refs. 41 and 42 and is contained in the supplementary material.

Time profiles of the electrical conductivity are qualitatively the same for all investigated HEs of composition $C_aH_bN_cO_d$, except for the cases of high-density TNT[43] and TATB-based HEs.[44] Figure 2 shows the typical electrical conductivity profile in the example of PETN with the density $\rho = 1.72$ g/cm^3. There is an increase behind the front to the maximum value denoted as σ_{max} followed by a rapid decrease to the point denoted as σ_{CJ}, which we relate to the end of the reaction zone (CJ-point). Then, the decrease becomes less steep, which is related spatially to the Taylor rarefaction wave. The gradients in the reaction zone and in the Taylor wave differ by two orders of magnitude allowing us to easily distinguish the boundary between zones. The coordinate of the profile x is related to the time t measured from the moment of the passage of the front by the ratio $x = Dt$, where D is the detonation velocity.

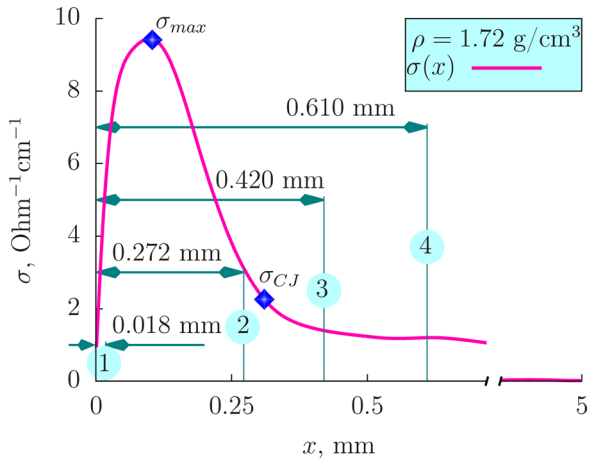

FIG. 2. Time profile of electrical conductivity at detonation of PETN with density $\rho = 1.72$ g/cm^3, and duration of high conductivity zone $0 < t < t(\sigma_{CJ})$ is 38 ns. Data related to marks are listed in Table I.

In Refs. 45–53, based on a large database of experimental data on electrical conductivity, the contact mechanism of conductivity by carbon structures is proved. These structures are formed immediately behind the detonation front in the chemical peak region and then evolve due to chemical reactions with carbon.

The method of conductivity is able to measure $\sigma(x)$ with the resolution on par with the most precise methods.[35,39,54–56] In Refs. 49 and 57, the jump of conductivity occurring in less than 6 ns was registered.

The model of electric conductivity agrees with the data on the fast carbon condensation and the early formation of diamond nuclei obtained in Refs. 37 and 59–62. The author of Ref. 63 writes about the formation of the carbon skeleton with the simultaneous displacement of "alien" elements. The presence of carbon fibers in preserved detonation products is confirmed by the results of Refs. 64–67. In carbon-rich HEs, elongated conductive carbon fibers were found and structure bifurcation points.[68] In Refs. 69 and 70, the reconstruction was performed of fractal aggregates consisting of detonation nanodiamond (DND) particles of different sizes. The simulation by the Monte Carlo method was carried out with the distribution of DND size obtained by the high-resolution transmission electron microscopy. The results on the intensity of one-dimensional small-angle x-ray scattering were also taken into account. Branched carbon structures were obtained.

Hence, electrical conductivity is a sensitive tool for the diagnostics of the chemical state of the matter in the detonation process.

III. COMPARISON WITH EXPERIMENTAL AND SIMULATION DATA

A. Comparison of the electrical conductivity profile with the data of different experimental methods

It is interesting to compare different methods with the electrical conductivity, which reflects the evolution of the conductive form of carbon. Table I shows the results of the investigations of the detonation of PETN with different charge structures: agitated, single crystal, pressed to different densities, and powder.[35,39,54–56,71,72] The numbers correspond to the marks in Fig. 2. In Refs. 54–56, only the duration of the reaction zone is given. For the sake of correctness, we recalculate the duration to the width using the formula $X_J = (D - \langle U \rangle)t_J$. Here, $\langle U \rangle$ is the average mass velocity inside the chemical peak, D is the detonation velocity, and t_J is the duration of chemical reaction. The width corresponding to mark 1 is close to the increase in $\sigma(x)$, and it can be related to the reaction stage indistinguishable by some experimental methods. The inflection point σ_{CJ}, which we relate to the CJ-point is close to marks 2, 3, and 4.

In the experimental data presented, a large variation is observed in the duration of the reaction zone—from 3 to 95 ns. This may be due to different charge structures that affect the chemical peak. In this case, the annotated one, as highly homogeneous, should have a duration close to that observed for a single crystal. However, the difference

Published under an exclusive license by AIP Publishing

TABLE I. Duration of chemical reaction t_J at detonation of PETN with different charge structures.

N	ρ, g/cm^3	$d \times L$, mm	t_J, ns	P_{CJ}, GPa	State	Ref.
1	1.53	ø 13.6–25 × 5–30	3	25.63	PETN/binder 83/17	54
	1.53	ø 120 × 40–100	4	23.2	PETN/binder 83/17	71
	1.65	ø 32 × 11	7 ± 2	26.1 ± 0.6	PETN/binder 95/5	56
	1.74	ø 40 × 80	<5	≈30	Agated	55
	1.76	ø 25.4 × 10	<5	31.5	Pressed	35
2	1.77	ø 20–30 × 50	≈ 50	≈30	Pressed	72
3	1.73	ø 40 × 40	80 ± 20	30.5	Pressed	55
4	1.77	ø 14 ×6–14	95	28	Single crystal (100)	39

between these two measurements is maximal, which indicates significant methodological difficulties in studying the reaction zone with "mechanical" characteristics. For pressed charges with a close density ($\rho = 1.73$–1.77 g/cm^3), there is also a significant difference from 5 to 80 ns. A possible explanation for this discrepancy may be the assumption that different stages of the chemical reaction were taken as the end of the reaction zone, which is reflected in the electrical conductivity profile.

B. Duration of a chemical reaction. Comparison of experimental data on the electrical conductivity with the results of simulations based on the Arrhenius kinetics

Here, we perform the comparison of the duration of the high electrical conductivity zone with the results of the most known chemical-kinetics models based on the Arrhenius kinetics for the case of detonating HMX.

Figure 3 presents the data on the reaction zone duration τ vs the hot-spot temperature T_{hs} according to the simulation data of

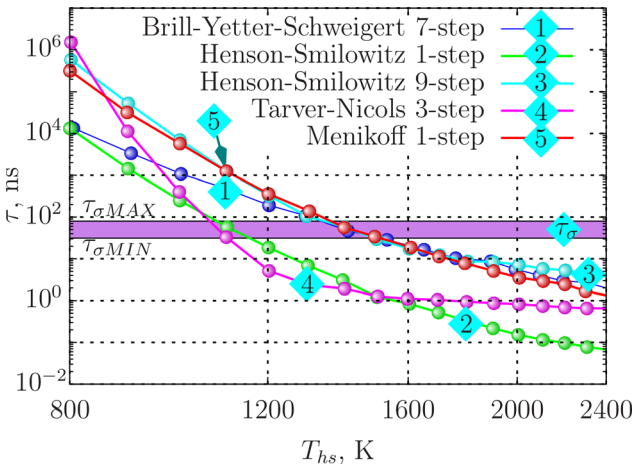

FIG. 3. Dependence of the reaction zone duration τ on the hot-spot temperature in HMX, simulation results: Henson–Smilowitz one-step model,[73] Menikoff one-step model,[74] Tarver–Nichols three-step model,[75] Henson Smilowitz nine-step model,[76] and Brill–Yetter–Schweigert seven-step model;[19] τ_σ—range of the duration of the high conductivity zone in detonating HMX of density from 1.3 to 1.9 g/cm^3.

Refs. 19 and 73–76. The dependence is of a sharp exponential type $\frac{1}{\tau} = A \exp^{-B/RT_{hs}}$ (A and B are model constants). The whole possible temperature range is covered. For comparison, the experimental data are shown on the duration of the high conductivity zone $\tau_{\sigma MIN}$ and $\tau_{\sigma MAX}$ at the detonation of HMX with densities from the powder one to the maximum obtained by pressing, the region between them is shaded. Table II presents the data on τ_σ vs density ρ_0 for different grain sizes and the estimate of pressure according to the formula $P_{CJ} = \rho_0 D^2/4$. One can see that the duration τ_σ only slightly depends on density, temperature, and pressure but is sensitive to the grain size $\langle d \rangle$. With the increase in density, the substance becomes more uniform; therefore, the duration of the reaction zone becomes close to the one for a substance of powder density with small grains. Thus, the concentration of hot spots influences the reaction zone more strongly than the values of pressure and temperature.[48] The influence of the grain size on the chemical peak was obtained in Refs. 72 and 77–81. The relation between the grain size and the sensitivity is known.[82–84] In Ref. 85, the critical thickness decreased to very small values (700 μm for TATB, 20 μm for sensitive benzotrifuroxan) for a planar layer of HE produced by the thermal vacuum sublimation, i.e., with heterogeneities at the nanoscale.

In our opinion, the development of an alternative for the available kinetics is necessary to explain the dependence of the reaction zone on the concentration of hot spots under a weak influence of pressure.

TABLE II. Duration of the high conductivity zone $\langle \tau_\sigma \rangle$ (average value) at density ρ_0, pressure P_{CJ}, and temperature T_{CJ} in CJ-point, correspondingly, $\langle d \rangle$—average HE grain size, date from the works.[53,58,77,78]

HE	ρ_0, g/cm^3	$\langle d \rangle$, μm	P_{CJ}, GPa	T_{CJ}, K	$\langle \tau_\sigma \rangle$, ns
RDX	1.2	11	12	4000	31
RDX	1.2	160	12	4000	56
RDX	1.7	160	31	3550	48
HMX	1.3	21	15	3950	34
HMX	1.3	430	15	3950	63
HMX	1.8	430	34	3500	42
PETN	1.1	80	9	4100	59
PETN	1.1	260	9	4100	92
PETN	1.7	260	29	3700	44

Published under an exclusive license by AIP Publishing

IV. DISCUSSION

The mechanism responsible for triggering a chemical reaction in a detonation wave can also manifest itself during the transition from shock to detonation.

There are at present two concepts of the explosion inception under the impact: thermal and non-thermal.[30] In the non-thermal theory, the cause of the initiation is the activation and the breaking of chemical bonds due to the relative shear of the molecules, the breaking of chemical bonds due to the plastic deformation,[86,87] the overheating of translational degrees of freedom in the shock front and the consequent bond breaking,[88] and the atomization of HE molecules in the narrow (20–100 Å) shock front region due to high gradients of pressure and velocity.[89,90] Despite the difference in detail, the authors agree with the opinion that the breaking of chemical bonds occurs not due to heating but the high-intense impact. According to the thermal concept, the mechanical impact leads to the collapse of pores and point heating up at the inhomogeneities.[4–11,14–19] The thermal destruction then leads to the inception of fast chemical reactions. The same mechanism is used for explaining the course of reaction during the detonation process: there is a compression of matter in the detonation wave leading to heating and the chemical reaction.[30] Thus, a high temperature is the starting mechanism. The comparison of the simulation results based on the thermal mechanism and the experimental data of electric conductivity listed in the previous paragraph demonstrates irreducible discrepancies.

Let us consider the development of the reaction at the shock-wave impact on a structured dense medium.

In the investigation of HE single crystals, anisotropy of the shock-wave sensitivity was observed for PETN,[86,91] RDX,[92] HMX,[93] and TATB.[94] For PETN, this anisotropy is most pronounced.

Table III shows the results of the investigations of Dick *et al.*,[86] Yoo *et al.*,[91] and Cawkwell *et al.*[95] on the shock-wave sensitivity, and the distance of the detonation inception h is listed. The initiation pressure for highly and low sensitive directions of the PETN single crystals are 4.2 and 19.5 GPa, correspondingly. The values of pressure differ by the factor of 4.6, which exceeds sufficiently the experimental error. Dick claims in Ref. 96 that at the shock loading of a PETN single crystal, a uniaxial compression occurs. A two-wave configuration is observed, which degenerates to a single-wave one at the increasing impact—at the detonation. Dick explains the high sensitivity of a PETN single crystal in the ⟨110⟩ direction by breaking the chemical bonds due to the steric hindrance to shear at the molecular level. At the porosity of 3.26% (line 5 of Table III) and chaotic crystal orientation, the necessary initiation pressure decreases twofold compared to the highly sensitive direction (line 2 of Table III). This means that there is a strong dependence on the hot-spot concentration similar to Table II, and there are no hot spots in an ideal single crystal.

TABLE III. Reaction development in PETN in different crystal states.

N	ρ, g/cm^3	Condition	P, GPa	Orientation	Notes	Ref.
1	1.778	Single crystal	3.95	⟨110⟩	No detonation	86
2	1.778	Single crystal	4.2	⟨110⟩	Transition to detonation	86
3	1.778	Single crystal	19.5	⟨100⟩	No detonation	86
4	1.774	Single crystal	35.4	⟨100⟩	Detonation	71
5	1.72	Pressed powder	2		Transition to detonation	30

References 39 and 71 mention different shapes of the mass velocity profile reflecting the reaction course at the detonation of single crystals in different directions. Dick measured the mass velocity at the shock impact and its profiles depended on the single crystal orientation.[96] The different reaction velocity in different directions was observed even in a slow deflagration process.[97]

From the ZND model,[1–3,98] one can estimate the density of detonating substance at the moment of maximum compression, i.e., in the von Neumann peak. According to the data of Ref. 71, the maximum pressure at the detonation of PETN single crystals with the initial density $\rho_0 = 1.774$ g/cm^3 is equal to $P_N = 35.4$ GPa, and the detonation velocity is $D = 8.3$ km/s. This gives us the density in the von Neumann peak ρ_N expressed through the initial one as

$$\rho_N = \frac{\rho_0}{1 - \dfrac{P_N}{\rho_0 D^2}} \approx 1.41\rho_0.$$

The detonation wave passes a molecule of PETN[99] is $\frac{L}{D} = \frac{9.3\times10^{-10}}{8.3\times10^{3}} \approx 10^{-13}$ s, which is comparable to the oscillation period of intermolecular bonds. Thus, the uniaxial compression of a molecule by 40% in a time of a single atomic oscillation leads, in our opinion, to the strong deformation of intramolecular bonds along the selected direction. Such deformation brings the molecules out from the equilibrium state. For a metastable substance, such as HE, this should lead to the inception of the chemical reaction.

The strong compression can also lead to the formation of intermolecular bonds similar to the observed polymerization of hydrocarbons with benzene rings at pressures of tens of kilobars.[100] The diamond formation from pyrolytic graphite resulting from the bond rearrangement during the action of a shock wave was obtained in Refs. 101 and 102 with the necessary pressure larger than 20 GPa. The relation between the orientation of graphite and the final state of nanodiamonds was revealed in Ref. 103.

The mechanism responsible for the reaction development in a single crystal of HE under the shock-wave impact may be operational also at the propagation of detonation. It is not the only one, but it makes a decisive contribution to the reaction course in polycrystal media.

Thus, under a high-intensity impact on a single crystal, uniaxial compression occurs, and the substance is compressed in the selected direction by about 50%, which leads to the destruction and rearrangement of intra- and intermolecular bonds. This process is accompanied by the energy release with initiates the chemical reaction in the material. The bonds normal to this direction are less affected and are partially preserved.

The assumption of incomplete destruction of HE molecules was made in Refs. 88, 104, and 105. In Ref. 88, the assumption was made that translational degrees of freedom are overheated in the shock front leading to the concentration of energy in the most stiff bonds, which leads to only their breakup. The author of Ref. 63 claims that the total

Published under an exclusive license by AIP Publishing

destruction of HE molecules does not occur, and the construction of a carbon skeleton proceeds with a gradual displacement of alien elements, which cover the surface of the carbon skeleton. The existence of such an "envelop" is beyond the doubts. There are experimental data in Refs. 59 and 106–111 on the presence of bonds between the carbon of nanodiamonds and the atoms of N, O, H, and functional groups. We assume that these are fragments of HE molecules and not the result of a chemical reaction in the detonation wave.

In a porous inhomogeneous matter, a polycrystalline powder, the rearrangement of chemical bonds starts at the points of grain contact, where the zones of locally increased pressure are formed. The reaction incepts at the surface where the HE molecules are in the dedicated position relative to inner ones.

Thus, the description proposed is in agreement with experimental data on the anisotropy of the shock-wave sensitivity with the results of the investigation by the tracer atoms method, with the experimental data on the impact load of HEs of different structures, and with the analysis of preserved detonation products. Using this kinetics, it is possible to explain the formation of penetrating conductive structures in tens of nanoseconds and the following decrease when the high conductivity region corresponds to the reaction zone.

In the framework of this hypothesis, the hot spots[30] do not occur in voids. Instead, they are generated at the places of the contact of microcrystals, where elevated local pressure is produced in the shock front which is sufficient to initiate the chemical reaction. This is confirmed by the data of Refs. 112 and 113, where it was obtained that the chemical reaction in the HMX single crystal develops from hot spots generated mainly at sharp angles and at the contacts between grains, i.e., in the zones of the local pressure increase. The authors of Ref. 33 conclude based on the simulated collision of two PETN molecules that the key role is played by mechanical processes and not by the temperature increase during the compression along the shock adiabatic. With such a mechanism of reaction development, there should be a strong dependence of the duration of the reaction zone on the grain size, which is indeed observed (Table II).

V. CONCLUSION

Experimental data on the study of the reaction zone of detonating condensed explosives are compared with the data on the electrical conductivity. The discrepancy in the duration of the reaction zone obtained from the mechanical parameters can be explained by fixing different stages of the chemical reaction. A comparison of the results on the electrical conductivity and the numerical experiment clearly shows that in order to explain this rapid response, it is necessary to involve a non-thermal concept of reaction development under shock.

SUPPLEMENTARY MATERIAL

See the supplementary material for the description of an experimental scheme for investigating the electrical conductivity of detonating condensed explosives.

ACKNOWLEDGMENTS

This research was funded by the Ministry of Science and Higher Education of the Russian Federation (Project No. 075-15-2020-781).

AUTHOR DECLARATIONS

Conflict of Interest

The authors have no conflicts to disclose.

Author Contributions

Nataliya P. Satonkina: Conceptualization (lead); Data curation (lead); Formal analysis (lead); Investigation (lead); Resources (lead); Supervision (lead); Visualization (lead); Writing – original draft (lead); Writing – review and editing (equal). **Dmitry Medvedev:** Formal analysis (supporting); Investigation (supporting); Writing – original draft (supporting); Writing – review and editing (equal).

DATA AVAILABILITY

The data that support the findings of this study are available from the corresponding author upon reasonable request.

REFERENCES

[1]Y. B. Zel'dovich, "On the theory of the propagation of detonation in gaseous systems," ("K teorii rasprostraneniya detonatsii v gazoobraznykh sistemakh"), J. Exp. Teor. Phys. **10**, 542–568 (1940) (in Russian).
[2]J. von Neumann, "Theory of detonation waves (OD-2)," Report No. Division B-1/Serial N 238 (National Defence Research Committee of the Office of Scientific Research and Development, 1942).
[3]W. Döring, "Über den detonationsvorgang in gasen," Ann. Phys. **435**, 421–436 (1943).
[4]B. A. Khasainov, A. V. Attetkov, and A. A. Borisov, "Shock-wave initiation of porous energetic materials and visco-plastic model of hot spots," Chem. Phys. Rep. **15**(7), 987–1062 (1996) (in Russian).
[5]C. A. Handley, B. D. Lambourn, N. J. Whitworth, H. R. James, and W. J. Belfield, "Understanding the shock and detonation response of high explosives at the continuum and meso scales," Appl. Phys. Rev. **5**(1), 011303 (2018).
[6]N. K. Bourne and A. M. Milne, "The temperature of a shock-collapsed cavity," Proc. R. Soc. A **459**(2036), 1851–1861 (2003).
[7]M. A. Wood, D. E. Kittell, C. D. Yarrington, and A. P. Thompson, "Multiscale modeling of shock wave localization in porous energetic material," Phys. Rev. B **97**(1), 014109 (2018).
[8]E. M. Escauriza, J. P. Duarte, D. J. Chapman, M. E. Rutherford, L. Farbaniec, J. C. Jonsson, L. C. Smith, M. P. Olbinado, J. Skidmore, P. Foster, T. Ringrose, A. Rack, and D. E. Eakins, "Collapse dynamics of spherical cavities in a solid under shock loading," Sci. Rep. **10**(1), 8455 (2020).
[9]M. P. Kroonblawd and R. A. Austin, "Sensitivity of pore collapse heating to the melting temperature and shear viscosity of HMX," Mech. Mater. **152**, 103644 (2021).
[10]R. A. Austin, N. R. Barton, W. M. Howard, and L. E. Fried, "Modeling pore collapse and chemical reactions in shock-loaded HMX crystals," J. Phys. Conf. Ser. **500**(PART 5), 052002 (2014).
[11]H. K. Springer, S. Bastea, A. L. Nichols III, C. M. Tarver, and J. E. Reaugh, "Modeling the effects of shock pressure and pore morphology on hot spot mechanisms in HMX," Propellants Explos. Pyrotech. **43**(8), 805–817 (2018).
[12]S. Roy, B. P. Johnson, X. Zhou, Y. T. Nguyen, D. D. Dlott, and H. S. Udaykumar, "Hot spot ignition and growth from tandem micro-scale simulations and experiments on plastic-bonded explosives," J. Appl. Phys. **131**(20), 205901 (2022).
[13]B. W. Hamilton, M. P. Kroonblawd, and A. Strachan, "The potential energy hotspot: Effects of impact velocity, defect geometry, and crystallographic orientation," J. Phys. Chem. C **126**(7), 3743–3755 (2022).
[14]C. Li, B. W. Hamilton, and A. Strachan, "Hotspot formation due to shock-induced pore collapse in 1,3,5,7-tetranitro-1,3,5,7-tetrazoctane (HMX): Role of pore shape and shock strength in collapse mechanism and temperature," J. Appl. Phys. **127**(17), 175902 (2020).
[15]K. Zhong, R. Bu, F. Jiao, G. Liu, and C. Zhang, "Toward the defect engineering of energetic materials: A review of the effect of crystal defects on the sensitivity," Chem. Eng. J. **429**, 132310 (2022).

Published under an exclusive license by AIP Publishing

[16]V. S. Solov'ev, "Some specific features of shock-wave initiation of explosives," Combust. Explos. Shock Waves **36**(6), 734–744 (2000).
[17]M. P. Kroonblawd and L. E. Fried, "High explosive ignition through chemically activated nanoscale shear bands," Phys. Rev. Lett. **124**(20), 206002 (2020).
[18]P. Das, P. Zhao, D. Perera, T. Sewell, and H. S. Udaykumar, "Molecular dynamics-guided material model for the simulation of shock-induced pore collapse in β-octahydro-1,3,5,7-tetranitro-1,3,5,7-tetrazocine (β-HMX)," J. Appl. Phys. **130**(8), 085901 (2021).
[19]N. K. Rai, S. P. Koundinyan, O. Sen, I. V. Schweigert, B. F. Henson, and H. S. Udaykumar, "Evaluation of reaction kinetics models for meso-scale simulations of hotspot initiation and growth in HMX," Combust. Flame **219**, 225–241 (2020).
[20]N. K. Rai, E. M. Escauriza, D. E. Eakins, and H. S. Udaykumar, "Mechanics of shock induced pore collapse in poly(methyl methacrylate) (PMMA): Comparison of simulations and experiments," J. Mech. Phys. Solids **143**, 104075 (2020).
[21]M. J. Cawkwell and V. W. Manner, "Ranking the drop-weight impact sensitivity of common explosives using Arrhenius chemical rates computed from quantum molecular dynamics simulations," J. Phys. Chem. A **124**, 74–81 (2020).
[22]G. Chu, Z. Yang, T. Xi, J. Xin, Y. Zhao, W. He, M. Shui, Y. Gu, Y. Xiong, and T. Xu, "Relaxed structure of typical nitro explosives in the excited state: Observation, implication and application," Chem. Phys. Lett. **698**, 200–205 (2018).
[23]V. I. Pepekin, B. L. Korsunskii, and A. A. Denisaev, "Initiation of solid explosives by mechanical impact," Combust. Explos. Shock Waves **44**, 586–590 (2008).
[24]S. V. Bondarchuk, "Impact sensitivity of aryl diazonium chlorides: Limitations of molecular and solid-state approach," J. Mol. Graph. Modell. **89**, 114–121 (2019).
[25]V. W. Manner, M. J. Cawkwell, E. M. Kober, T. W. Myers, G. W. Brown, H. Tian, C. J. Snyder, R. Perriot, and D. N. Preston, "Examining the chemical and structural properties that influence the sensitivity of energetic nitrate esters," Chem. Sci. **9**, 3649–3663 (2018).
[26]M. J. Cawkwell, R. Perriot, N. Lease, and V. W. Manner, "Systematic study of the explosive chemical kinetics of derivatives of ETN and PETN at low pressure," AIP Conf. Proc. **2272**, 070006 (2020).
[27]C. Lin and K. H. Luo, "Kinetic simulation of unsteady detonation with thermodynamic nonequilibrium effects," Combust. Explos. Shock Waves **56**, 435–443 (2020).
[28]H. Zheng and M. Yu, "Thermodynamically consistent detonation model for solid explosives," Combust. Explos. Shock Waves **56**, 545–555 (2020).
[29]B. Stimac, H. Y. S. Chan, M. Kunzel, and M. Suceska, "Numerical modelling of detonation reaction zone of nitromethane by EXPLO5 code and Wood and Kirkwood theory," Cent. Euro. J. Energy Mater. **17**, 239–261 (2020).
[30]S. G. Andreev, A. V. Babkin, F. A. Baum, N. A. Imkhovik, I. F. Kobylkin, V. I. Kolpakov, S. V. Ladov, V. A. Odintsov, L. P. Orlenko, V. N. Okhitin, V. V. Selivanov, V. S. Solov'ev, V. P. Chelyshev, K. P. Stanyukovich, and B. I. Shekhter, Physics of Explosion [Fizika Vzryva] (Fizmatlit, Moscow, 2004), Vol. 1, p. 832 (in Russian).
[31]T. R. Botcher and C. A. Wight, "Transient thin film laser pyrolysis of RDX," J. Phys. Chem. **97**, 9149–9153 (1993).
[32]X. Zhao, E. J. Hintsa, and Y. T. Lee, "Infrared multiphoton dissociation of RDX in a molecular beam," J. Chem. Phys. **88**, 801–810 (1988).
[33]A. C. Landerville, I. I. Oleynik, and C. T. White, "Reactive molecular dynamics of hypervelocity collisions of PETN molecules," J. Phys. Chem. A **113**, 12094–12104 (2009).
[34]V. Stepanov, V. Anglade, W. A. Balas Hummers, A. V. Bezmelnitsyn, and L. N. Krasnoperov, "Production and sensitivity evaluation of nanocrystalline RDX-based explosive compositions," Propellants Explos. Pyrotech. **36**, 240–246 (2011).
[35]C. M. Tarver, "Multiple roles of highly vibrationally excited molecules in the reaction zones of detonation waves," J. Phys. Chem. A **101**, 4845–4851 (1997).
[36]C. M. Tarver and T. D. Tran, "Thermal decomposition models for HMX-based plastic bonded explosives," Combust. Flame **137**, 50–62 (2004).
[37]V. F. Anisichkin, "On the mechanism of the detonation of organic high explosives," Russ. J. Phys. Chem. B **10**, 451–455 (2016).
[38]Y. Li, R. K. Kalia, A. Nakano, K.-I. Nomura, and P. Vashishta, "Multistage reaction pathways in detonating high explosives," Appl. Phys. Lett. **105**, 204103 (2014).
[39]A. V. Fedorov, A. L. Mikhailov, L. K. Antonyuk, D. V. Nazarov, and S. A. Finyushin, "Determination of parameters of detonation waves in PETN and HMX single crystals," Combust. Explos. Shock Waves **47**, 601–605 (2011).
[40]M. S. Powell, M. N. Sakano, M. J. Cawkwell, P. R. Bowlan, K. E. Brown, C. A. Bolme, D. S. Moore, S. F. Son, A. Strachan, and S. D. McGrane, "Insight into the chemistry of PETN under shock compression through ultrafast broadband mid-infrared absorption spectroscopy," J. Phys. Chem. A **124**, 7031–7046 (2020).
[41]A. P. Ershov, N. P. Satonkina, and G. M. Ivanov, "High-resolution conductivity profile measurements in detonating pressed explosive," Tech. Phys. Lett. **30**, 1048–1050 (2004).
[42]A. P. Ershov, N. P. Satonkina, and G. M. Ivanov, "Electroconductivity profiles in dense high explosives," Russ. J. Phys. Chem. B **1**, 588–599 (2007).
[43]A. P. Ershov and N. P. Satonkina, "Investigation of the reaction zone in heterogeneous explosives substances using an electrical conductivity method," Combust. Explos. Shock Waves **45**, 205–210 (2009).
[44]N. P. Satonkina and I. A. Rubtsov, "Electrical conductivity distribution during detonation of a TATB–based explosive," Tech. Phys. **61**, 142–145 (2016).
[45]A. P. Ershov, N. P. Satonkina, A. V. Plastinin, and A. S. Yunoshev, "Diagnostics of the chemical reaction zonein detonation of solid explosives," Combust. Explos. Shock Waves **56**, 705–715 (2020).
[46]N. P. Satonkina, A. P. Ershov, A. V. Plastinin, and A. S. Yunoshev, "Chemical reaction zone and electrical conductivity profile in detonating high explosives," Combust. Flame **206**, 249–251 (2019).
[47]N. P. Satonkina, "Chemical composition of detonation products of condensed explosives and its relationship to electrical conductivity," J. Phys.: Conf. Ser. **946**, 012059 (2018).
[48]N. P. Satonkina, "Duration of the zone of high electrical conductivity at the detonation of RDX of different densities," J. Phys.: Conf. Ser. **894**, 012136 (2017).
[49]N. Satonkina, A. Ershov, A. Kashkarov, A. Mikhaylov, E. Pruuel, I. Rubtsov, I. Spirin, and V. Titova, "Electrical conductivity distribution in detonating benzotrifuroxane," Sci. Rep. **8**, 9635 (2018).
[50]N. P. Satonkina, "The dynamics of carbon nanostructures at detonation of condensed high explosives," J. Appl. Phys. **118**, 245901 (2015).
[51]N. P. Satonkina, "Correlation of electrical conductivity in the detonation of condensed explosives with their carbon content," Combust. Explos. Shock Waves **52**, 488–492 (2016).
[52]N. P. Satonkina and D. A. Medvedev, "On the mechanism of carbon nanostructures formation at reaction of organic compounds at high pressure and temperature," AIP Adv. **7**(8), 085101 (2017).
[53]N. P. Satonkina, "Influence of the grain size of high explosives on the duration of a high conductivity zone at the detonation," Sci. Rep. **9**, 12256 (2019).
[54]A. V. Fedorov, A. V. Menshikh, and N. B. Yagodin, "Structure of a detonation front in heterogeneous high explosives (HE)," Chem. Phys. Rep. **18**, 2129–2138 (2000).
[55]B. G. Loboiko and S. N. Lubyatinsky, "Reaction zones of detonating solid explosives," Combust. Explos. Shock Waves **36**, 716–733 (2000).
[56]H. Pei, W. Huang, X. Zhang, and X. Zheng, "Measuring detonation wave profiles in plastic–bonded explosives using PDV," AIP Adv. **9**, 015306 (2019).
[57]N. P. Satonkina and A. P. Ershov, "Dynamics of carbon nanostructures in the benzotrifuroxan detonation," J. Phys.: Conf. Ser. **1787**, 012015 (2021).
[58]K. Tanaka, "Detonation properties of condensed explosives computed using the Kihara–Hikita–Tanaka equation of state," National Chemical Laboratory for Industry, Tsukuba Research Center (Tsukuba, Japan, 1983), p. 304.
[59]V. Yu.V. Yu. Dolmatov, A. N. Ozerin, I. I. Kulakova, O. O. Bochechka, N. M. Lapchuk, V. Myllymaki, and A. Vehanen, "Detonation nanodiamonds: New aspects in the theory and practice of synthesis, properties and applications," Russ. Chem. Rev. **89**, 1428–1462 (2020).
[60]V. F. Anisichkin, "Isotope studies of detonation mechanisms of TNT, RDX, and HMX," Combust. Explos. Shock Waves **43**, 580–586 (2007).
[61]J. A. Hammons, M. H. Nielsen, M. Bagge-Hansen, S. Bastea, C. May, W. L. Shaw, A. Martin,Y. Li, N. Sinclair, L. M. Lauderbach, R. L. Hodgin, D. A.

Published under an exclusive license by AIP Publishing

Orlikowski, L. E. Fried, and T. M. Willey, "Submicrosecond aggregation during detonation synthesis of nanodiamond," J. Phys. Chem. Lett. **12**, 5286–5293 (2021).
[62]V. Yu. Dolmatov, A. N. Ozerin, A. Vehanen, V. Myllymäki, and A. O. Dorokhov, "On the mechanism of formation of detonation diamonds," J. Superhard Mater. **43**(5), 330–335 (2021).
[63]O. N. Breusov, "On the question of the mechanism of dynamic synthesis of diamond from organic substances," Khim. Fiz. **21**, 110–112 (2002) (in Russian).
[64]Y. Nomura and K. Kawamura, "Soot derived from the detonation of a trinitrotoluene charge," Carbon **22**, 189–191 (1984).
[65]N. R. Greiner, D. S. Phillips, J. D. Johnson, and F. Volk, "Diamonds in detonation soot," Nature **333**, 440–442 (1988).
[66]X. Tao, X. Kang, and Z. Jiazheng, "Tem and hrem studies on ultradispersed diamonds containing soot formed by explosive detonation," Mater. Sci. Eng. B **38**, L1–L4 (1996).
[67]A. O. Kashkarov, E. R. Pruuel, K. A. Ten, I. A. Rubtsov, E. Y. Gerasimov, and P. I. Zubkov, "Transmission electron microscopy and X-ray diffraction studies of the detonation soot of high explosives," J. Phys.: Conf. Ser. **774**, 012072 (2016).
[68]N. P. Satonkina, A. P. Ershov, A. O. Kashkarov, and I. A. Rubtsov, "Elongated conductive structures in detonation soot of high explosives," RSC Adv. **10**, 17620–17626 (2020).
[69]P. Kowalczyk, E.-Z. Piña-Salazar, J. K. Kirkensgaard, A. P. Terzyk, R. Futamura, T. Hayashi, E. Osawa, K. Kaneko, and A. Ciach, "Reconstructing the fractal clusters of detonation nanodiamonds from small–angle X-ray scattering," Carbon **169**, 349–356 (2020).
[70]A. N. Ozerin, T. S. Kurkin, L. A. Ozerina, and V. Y. Dolmatov, "X-ray diffraction study of the structure of detonation nanodiamonds," Crystallogr. Rep. **53**, 60–67 (2008).
[71]A. V. Fedorov, A. L. Mikhailov, L. K. Antonyuk, D. V. Nazarov, and S. A. Finyushin, "Determination of chemical reaction zone parameters, Neumann peak parameters, and the state in the Chapman–Jouguet plane in homogeneous and heterogeneous high explosives," Combust. Explos. Shock Waves **48**, 302–308 (2012).
[72]A. V. Utkin, V. M. Mochalova, A. I. Rogacheva, and V. V. Yakushev, "Structure of detonation waves in PETN," Combust. Explos. Shock Waves **53**, 199–204 (2017).
[73]B. F. Henson, B. W. Asay, L. B. Smilowitz, and P. M. Dickson, "Ignition chemistry in HMX from thermal explosion to detonation," AIP Conf. Proc. **620**, 1069–1072 (2002).
[74]R. Menikoff, "Detonation waves in PBX 9501," Combust. Theory Modell. **10**, 1003–1021 (2006).
[75]C. M. Tarver, S. K. Chidester, and A. L. Nichols III, "Critical conditions for impact- and shock-induced hot spots in solid explosives," J. Phys. Chem. **100**, 5794–5799 (1996).
[76]B. F. Henson, L. Smilowitz, J. J. Romero, and B. W. Asay, "Modeling thermal ignition and the initial conditions for internal burning in PBX 9501," AIP Conf. Proc. **1195**, 257–262 (2009).
[77]A. P. Ershov and N. P. Satonkina, "Electrical conductivity distributions in detonating low-density explosives—Grain size effect," Combust. Flame **157**, 1022–1026 (2010).
[78]A. P. Ershov, A. O. Kashkarov, E. R. Pruuel, N. P. Satonkina, V. V. Sil'vestrov, A. S. Yunoshev, and A. V. Plastinin, "Nonideal detonation regimes in low density explosives," J. Appl. Phys. **119**, 075903 (2016).
[79]V. Pichot, B. Risse, F. Schnell, J. Mory, and D. Spitzer, "Understanding ultrafine nanodiamond formation using nanostructured explosives," Sci. Rep. **3**, 2159 (2013).
[80]V. Pichot, M. Comet, B. Risse, and D. Spitzer, "Detonation of nanosized explosive: New mechanistic model for nanodiamond formation," Diamond Relat. Mater. **54**, 59–63 (2015).
[81]V. M. Mochalova, A. V. Utkin, and A. V. Anan'in, "Effect of the degree of dispersion on the detonation wave structure in pressed TNETB," Combust. Explos. Shock Waves **43**, 575–579 (2007).
[82]A. Y. Apin, "Influence of physical structure and aggregate state on detonability of high explosives," Dokl. Akad. Nauk SSSR **50**, 285–289 (1945) (in Russian).
[83]A. Y. Apin and L. N. Stesik, "Critical diameters of powdered high explosives. Physics of explosion" [Fizika vzryva]. Sbornik No. 3 (Izd-vo AN SSSR. pp. 87–92, 1955) (in Russian).
[84]B. A. Khasainov, B. S. Ermolaev, H.-N. Presles, and P. Vida, "On the effect of grain size on shock sensitivity of heterogeneous high explosives," Shock Waves **7**, 89–105 (1997).
[85]D. V. Mil'chenko, V. A. Gubachev, L. A. Andreevskikh, S. A. Vakhmistrov, A. L. Mikhailov, V. A. Burnashov, E. V. Khaldeev, A. I. Pyatoikina, S. S. Zhuravlev, and V. N. German, "Nanostructured explosives produced by vapor deposition: Structure and explosive properties," Combust. Explos. Shock Waves **51**, 80–85 (2015).
[86]J. J. Dick, R. N. Mulford, W. J. Spencer, D. R. Pettit, E. Garcia, and D. C. Shaw, "Shock response of pentaerythritol tetranitrate single crystals," J. Appl. Phys. **70**, 3572–3587 (1991).
[87]C. S. Coffey, "Initiation due to plastic deformation from shock or impact," Theor. Comput. Chem. **13**, 101–123 (2003).
[88]A. N. Dremin, "Discoveries in detonation of molecular condensed explosives in the 20th century," Combust. Explos. Shock Waves **36**, 704–715 (2000).
[89]F. E. Walker, "Physical kinetics," J. Appl. Phys. **63**, 5548–5554 (1988).
[90]F. E. Walker, "New support for physical kinetics," Chem. Phys. Rep. **17**, 31–36 (1998) (in Russian).
[91]C. S. Yoo, N. C. Holmes, P. C. Souers, C. J. Wu, F. H. Ree, and J. J. Dick, "Anisotropic shock sensitivity and detonation temperature of pentaerythritol tetranitrate single crystal," J. Appl. Phys. **88**, 70–75 (2000).
[92]N. Wang, J. Peng, A. Pang, J. Hu, and T. He, "Study on the anisotropic response of condensed-phase RDX under repeated stress wave loading via ReaxFF molecular dynamics simulation," J. Mol. Model. **22**, 229 (2016).
[93]X. Wang, Y. Wu, F. Huang, and L. Zhang, "Dynamic anisotropic response of β–HMX and α–RDX single crystals using plate impact experiments at 1 GPa," Propellants Explos. Pyrotech. **43**, 759–770 (2018). 2018.
[94]X. Huang, F. Guo, K. Yao, Z. Lu, Y. Ma, Y. Wen, X. Dai, M. Li, and X. Long, "Anisotropic hydrogen bond structures and orientation dependence of shock sensitivity in crystalline 1,3,5-tri-amino-2,4,6-tri-nitrobenzene (TATB)," Phys. Chem. Chem. Phys. **22**, 11956–11966 (2020).
[95]M. J. Cawkwell, N. Mohan, D. J. Luscher, and K. J. Ramos, "Dissociation of $\langle 111 \rangle$ dislocations on $\{1\bar{1}0\}$ in pentaerythritol tetranitrate," Philos. Mag. **99**, 1079–1089 (2019).
[96]J. J. Dick, "Anomalous shock initiation of detonation in pentaerythritol tetranitrate crystals," J. Appl. Phys. **81**, 601–612 (1997).
[97]O. V. Sergeev and A. V. Yanilkin, "Molecular dynamics simulation of combustion front propagation in a PETN single crystal," Combust. Explos. Shock Waves **50**, 323–332 (2014) (in Russian).
[98]K. K. Shvedov, "Some problems of detonation of condensed explosives," Khim. Fiz. **23**, 27–50 (2004) (in Russian).
[99]National Center for Biotechnology Information (2022). PubChem Substance Record for SID 134972963, 10L39TRG1Z, Source: ChemIDplus. Retrieved July 30, 2022 from https://pubchem.ncbi.nlm.nih.gov/substance/134972963.
[100]A. N. Dremin and L. V. Babare, "The shock wave chemistry of organic substances," AIP Conf. Proc. **78**, 363–381 (1982).
[101]D. J. Erskine and W. J. Nellis, "Shock-induced martensitic transformation of highly oriented graphite to diamond," J. Appl. Phys. **71**, 4882–4886 (1992).
[102]E. Stavrou, M. Bagge-Hansen, J. A. Hammons, M. H. Nielsen *et al.*, "Detonation-induced transformation of graphite to hexagonal diamond," Phys. Rev. B **102**, 104116 (2020).
[103]M. P. Kroonblawd and N. Goldman, "Mechanochemical formation of heterogeneous diamond structures during rapid uniaxial compression in graphite," Phys. Rev. B **97**, 184106 (2018).
[104]E. V. Mironov, E. A. Petrov, and A. Y. Korets, "From analysis of the structure of ultrafine diamond to the problem of its formation kinetics," Combust. Explos. Shock Waves **40**, 473–476 (2004).
[105]V. Y. Klimenko, "Multiprocessor detonation model (version 3)," Chem. Phys. Rep **17**, 13–30 (1998) (in Russian).
[106]V. Y.Dolmatov, "On elemental composition and crystal-chemical parameters of detonation nanodiamonds," J. Superhard Mater. **31**, 158–164 (2009).

Published under an exclusive license by AIP Publishing

[107]V. L. Kuznetsov, M. N. Aleksandrov, I. V. Zagoruiko, A. L. Chuvilin, E. M. Moroz, V. N. Kolomiichuk, V. A. Likholobov, P. M. Brylyakov, and G. V. Sakovitch, "Study of ultradispersed diamond powders obtained using explosion energy," Carbon **29**, 665–668 (1991).
[108]N. M. Kuznetsov, S. I. Belousov, R. A. Kamyshinsky, A. L. Vasiliev, S. N. Chvalun, E. B. Yudina, and A. Y. Vul, " Detonation nanodiamonds dispersed in polydimethylsiloxane as a novel electrorheological fluid: Effect of nanodiamonds surface," Carbon **174**, 138–147 (2021).
[109]A. Krüger, F. Kataoka, M. Ozawa, T. Fujino, Y. Suzuki, A. E. Aleksenskii, A. Ya. Vul', and E. Ōsawa, "Unusually tight aggregation in detonation nanodiamond: Identification and disintegration," Carbon **43**, 1722–1730 (2005).
[110]G. V. Sakovich, A. S. Zharkov, and E. A. Petrov, "Results of research into the physicochemical processes of detonation synthesis and nanodiamond applications," Nanotechnol. Russ. **8**, 581–591 (2013).
[111]A. Ya. Korets, E. V. Mironov, and E. A. Petrov, "IR spectroscopic study of the organic component of ultrafine diamond produced by detonation synthesis," Combust. Explos. Shock Waves **39**, 464–469 (2003).
[112]B. P. Johnson, X. Zhou, H. Ihara, and D. D. Dlott, "Observing hot spot formation in individual explosive crystals under shock compression," J. Phys. Chem. A **124**, 4646–4653 (2020).
[113]W. P. Bassett, B. P. Johnson III, L. Salvati, E. J. Nissen, M. Bhowmick, and D. D. Dlott, "Shock initiation microscopy with high time and space resolution," Propellants Explos. Pyrotech. **45**, 223–235 (2020).

Published under an exclusive license by AIP Publishing